Temperature and composition evolution of the phonon density of states in (Ba,K)(Pb,Bi,Sb)O_3 ceramic oxides

1992 J. Phys.: Condens. Matter 4 965

(http://iopscience.iop.org/0953-8984/4/4/007)

J. Phys.: Condens. Matter 4 (1992) 965–975. Printed in the UK

Temperature and composition evolution of the phonon density of states in (Ba,K)(Pb,Bi,Sb)O_3 ceramic oxides

Kosmas Prassides†, *Matthew J Rosseinsky*‡§, *A José Dianoux*|| and Peter Day||

† School of Chemistry and Molecular Sciences, University of Sussex, Brighton BN1 9QJ, UK

‡ Inorganic Chemistry Laboratory, Oxford University, Oxford 0X1 3QR, UK

|| Institut Laue–Langevin, 38042 Grenoble, France

Received 16 August 1991, in final form 9 October 1991

Abstract. The neutron-weighted phonon density of states of the superconducting $Ba_{0.6}K_{0.4}BiO_3$, $BaPb_{0.75}Bi_{0.25}O_3$ and $BaPb_{0.75}Sb_{0.25}O_3$ perovskites and their non-superconducting analogues, $BaPbO_3$ and $BaBiO_3$, have been measured by the neutron time-of-flight technique between 5 and 300 K. The spectra show very pronounced changes in the energies and intensities of the oxygen bending and breathing phonons, in sharp contrast to the more subtle situation encountered with the cuprate superconductors. There are also changes in the low-energy transfer region, reflecting the structural and electronic variations in the series. The results are consistent with the predictions of theoretical models for a primarily phonon-mediated mechanism for superconductivity.

1. Introduction

The discovery of superconducting copper oxide systems [1] has dramatically changed the traditional ideas about superconductivity. Despite the wealth of experimental and theoretical studies of the cuprates, the question of the pairing mechanism in these systems still remains open. One common structural feature, however, is the presence of layers of corner-sharing CuO_4 units; these can be strictly square planar (e.g. in the electron-doped systems $Nd_{2-x}Ce_xCuO_{4-\delta}$ [2, 3]), part of strongly elongated octahedral CuO_6 groups (e.g. in the hole-doped systems La_{2-x} $Sr_xCuO_{4-\delta}$ [4, 5] or square-pyramidal CuO_5 units (e.g. in $YBa_2Cu_3O_{7-\delta}$ [6] and the T^* phases $Nd_{2-x-y}Ce_xSr_yCuO_{4-\delta}$ [7]). Furthermore, all the parent compounds of the high-T_c copper oxides are characterised by strong antiferromagnetic exchange interactions; the Cu sublattice AF long-range order is, however, destroyed upon either hole- or electron-doping just before the onset of superconductivity [3, 4, 8, 9], indicating the intimate (albeit destructive) relationship between the magnetic and (super)conducting properties of the CuO_2 layers.

The participation of phonons in the pairing mechanism through conventional electron–phonon coupling has been disputed but it is clear from inelastic neutron scattering studies that there is little difference in the phonon density of states (DOS)

§ Current address: AT&T Bell Laboratories, Murray Hill, NJ 07974, USA.

0953-8984/92/040965+11$04.50

between the superconducting (e.g. $La_{1.85}Sr_{0.15}CuO_4$) and their parent (e.g. La_2CuO_4) compositions [10], with no indication of any high density of low-frequency phonons in the superconductor. In general, all the observed phonon anomalies, when comparing a superconducting oxide with its non-superconducting parent material, mainly affect the high energy part of the measured phonon DOS [11], i.e. those modes involving motion of the oxygen ligands. However, different types of oxygen vibrations appear to be affected for different families of high-T_c cuprate superconductors [12] and a possible correlation between the frequency range of the phonon anomalies and the superconducting transition temperatures has been suggested [12]. In contrast to these subtle differences in the cuprates, substantial phonon softenings of oxygen vibrations have been reported [13] for the perovskite superconductor $Ba_{0.6}K_{0.4}BiO_3$ (T_c = 30 K) [14] which contains no Cu ions. These findings, combined with tunnelling spectroscopy measurements [15], provide evidence for conventional phonon-mediated pairing mechanism in the bismuthate superconductors. Recent INS measurements [16] on ^{18}O isotopically substituted samples have provided further support for a phonon mechanism in contrast to earlier work which favoured electron pairing mediated by strong electronic excitations [17].

Three-dimensional perovskite bismuth oxide superconductors predate the high-T_c cuprates. They were first discovered in the $BaPb_{1-x}Bi_xO_3$ solid solutions, the maximum T_c of 13 K being attained for $x = 0.25$ [18]. Such unusually high T_c could only be produced because strong electron–phonon coupling existed since the density of states at the Fermi level was relatively low [19]. The more recent discovery of even higher T_cs in the potassium-doped $BaBiO_3$ system [14] naturally focused renewed attention on the pairing mechanism in these systems in comparison with the cuprate superconductors. Powder neutron diffraction studies [20] of the semiconducting $BaBiO_3$ oxide have shown the presence of two inequivalent Bi sites in the unit cell, resulting in two sets of differing Bi–O bond lengths. Thus the structure may be described in terms of altemating, corner-sharing BiO_6 octahedra with Bi–O short (2.12 Å) and long (2.28 Å) bonds, resulting in a perovskite superstructure of dimensions $\sqrt{2}a_p \times \sqrt{2}a_p \times 2a_p$. Consequently, $BaBiO_3$ is a mixed valency oxide [21] better represented as $BaBi_{0.5}^{III}Bi_{0.5}^{V}O_3$ showing the presence of a charge density wave (CDW) commensurate with the underlying lattice. Early structural work on $BaPb_{0.75}Bi_{0.25}O_3$ established its structure as tetragonal [22] with a single (Pb/Bi) site, indicating that metallic and superconducting behaviour is found in this system after the (Bi^{III},Bi^{V}) CDW has been suppressed. However, the crystal chemistry of this system is very sensitive to the preparative conditions employed and the existence of other polymorphs with a monoclinic structure and two (Pb/Bi) sites has recently been established [23]. In contrast, the crystal structure of $Ba_{0.6}K_{0.4}BiO_3$ has been reported as cubic [14] with both the CDW and the tilting distortion of the BiO_6 octahedra having been suppressed as a result of K doping.

Crucial to evaluating mechanisms based on electron–phonon coupling is a knowledge of the phonon DOS, and its evolution with temperature and composition. In this paper, we report and discuss high-resolution measurements of the phonon DOS of the superconducting oxides $Ba_{0.6}K_{0.4}BiO_3$ (T_c= 30 K) [14], $BaPb_{0.75}Bi_{0.25}O_3$ (T_c = 13 K) [18] and $BaPb_{0.75}Sb_{0.25}O_3$ (T_c= 3.5 K) [24] up to 100 meV using the neutron time-of-flight technique, at temperatures from 300 to 100 K. For comparison, we also report measurements for the non-superconducting reference compounds $BaPbO_3$ (metallic) and $BaBiO_3$ (semiconducting). Additional data were also collected for $Ba_{0.6}K_{0.4}BiO_3$ (and its parent $BaBiO_3$) at temperatures above and below the superconducting transi-

tion temperature. We compare and contrast our results with previous investigations of the phonon properties of the bismuthate superconductors by either inelastic neutron scattering or optical vibrational spectroscopy. Reichardt *et al* [25] have measured the phonon dispersion curves and DOS of $BaPb_{0.75}Bi_{0.25}O_3$ at room temperature, identifying low-frequency zone boundary rotational modes as well as the zone centre breathing and ferroelectric modes. Raman scattering studies by Sugai *et al* [26] have established the existence of a number of soft modes in the same superconducting oxide, while low-resolution measurements of the scattering law by Masaki *et al* [27] have provided evidence of differences in the high-energy part of the phonon spectrum between $BaPbO_3$ and $BaPb_{0.75}Bi_{0.25}O_3$. $Ba_{0.6}K_{0.4}BiO_3$ has been studied by Loong *et al* [13, 16] using inelastic neutron scattering at 15 K down to 15 meV and showing very pronounced differences in its phonon DOS when compared to $BaBiO_3$. Molecular dynamics calculations by the same authors generally agree with the experimental data, but predict additional features, especially at low energies, that necessitate measurements at higher resolution and lower energy transfers.

2. Experimental procedure

$BaPbO_3$ was prepared by a solution-based citrate sol–gel technique, using barium and lead nitrates as starting materials; firing temperatures of 400 °C (4 hours, flowing N_2) and 850 °C (48 hours, flowing O_2, one intermediate regrind) were used. A similar method was adopted for the preparation of $BaPb_{0.75}Bi_{0.25}O_3$ and $BaPb_{0.75}Sb_{0.25}O_3$. $BaBiO_3$ was synthesised by a solid state nitrate technique [18] with firing temperatures of 800 °C. The $Ba_{0.6}K_{0.4}BiO_3$ sample was prepared according to the ceramic procedure described by Hinks *et al* [14], which does not require melting of the reactants. Powder x-ray diffraction measurements confirmed that the samples were monophasic. Four-probe AC resistivity measurements established superconducting transition temperatures of 13.1 K for $BaPb_{0.75}Bi_{0.25}O_3$ and 30 K for $Ba_{0.65}K_{0.4}BiO_3$.

The inelastic neutron scattering measurements were performed at the Institut Laue–Langevin, Grenoble using two time-of-flight spectrometers: IN6, operating in neutron-energy-gain with incident neutron wavelength of 5.12 Å and IN4, in neutron-energy-loss with wavelength of 0.84 Å. Such a combination allowed us to record data both at low temperatures (5–45 K) with better resolution at high energy transfers (down-scattering mode, the instrumental energy resolution varying from 6 meV at 25 meV to 4 meV at 80 meV) and higher temperatures (100–300 K) with better resolution at low energy transfers (up-scattering mode, the instrumental energy resolution varying from 0.1 meV at 1 meV to 3.5 meV at 25 meV to 17 meV at 80 meV energy transfer). Data were collected as follows: $BaBiO_3$ (IN6, 300 K, 200 K, 100 K; IN4, 45 K, 5 K); $Ba_{0.6}K_{0.4}BiO_3$ (IN6, 300 K, 200 K, 100 K; IN4, 45 K, 5 K); $BaPbO_3$, $BaPb_{0.75}Bi_{0.25}O_3$ and $BaPb_{0.75}Sb_{0.25}O_3$ (IN6, 300 K). Corrections were made for the aluminium can contribution by running an empty sample can. Vanadium was used as calibrant, allowing determination of the relative efficiencies of the counters. The TOF spectra were collected over the full range of scattering angles (IN6, 10–115°; IN4, 10–97°) and in order to improve data statistics, they were summed, though with loss of momentum transfer resolution. Within the framework of the incoherent approximation [28], the spectral distribution function $P(\bar{\alpha}, \beta)$ is given by

$$P(\bar{\alpha}, \beta) = 2\beta \sinh\left(\frac{\beta}{2}\right)\left(\frac{S(Q,\omega)}{\bar{\alpha}}\right) \tag{1}$$

where $S(Q,\omega)$ is the uncorrected symmetrized scattering law and the dimensionless variables $\bar{\alpha}$ and β are related to momentum and energy transfer through

$$\bar{\alpha} = \frac{\hbar^2 Q^2}{2MkT} \qquad \beta = \frac{\hbar\omega}{kT} \tag{2}$$

where M is an average atomic mass. The spectral distribution function $P(\bar{\alpha},\beta)$ can be corrected for instrumental background, Debye–Waller and multiphonon contributions, using approximate analytic procedures in a self consistent manner [29]. This results in a corrected one-phonon spectral distribution $P_1(\bar{\alpha},\beta)$, from which the generalized or 'neutron-weighted' phonon DOS is obtained:

$$G(\omega) = \exp(2W)P_1(\bar{\alpha},\beta) \tag{3}$$

where $\exp(-2W)$ is the Debye–Waller attenuation factor. For polyatomic compounds like the present oxides, $G(\omega)$ is related to the partial phonon DOS $g_i(\omega)$ for each atom i through the expression

$$G(\omega) = \left[\sum_i \left(\frac{c_i\sigma_i}{m_i}\right)\right]^{-1} \sum_i \left(\frac{c_i\sigma_i}{m_i}\right) g_i(\omega) \tag{4}$$

where σ_i is the total neutron scattering cross section for atom i, m_i its mass and c_i its concentration $\left(\sum_i c_i = 1\right)$.

3. Results

The generalized ('neutron-weighted') phonon density of states $G(\omega)$ (equation (3)) of all the samples measured in up-scattering mode between 0 and 100 meV at 300 K are shown in figure 1. $BaBiO_3$, $Ba_{0.6}K_{0.4}BiO_3$ and $BaPb_{0.75}Bi_{0.25}O_3$ show PDOS which extend smoothly to $\approx$ 90 meV with some instrumental broadening contribution to the high-energy tail. In contrast, in our experiments, we found that our multiphonon and background corrections were incomplete for the $BaPbO_3$ and $BaPb_{0.75}Sb_{0.25}O_3$ samples. The reason was the presence of substantial incoherent contributions to the scattering, extending up to 150 meV, presumably because of adsorbed water; this hydrogen contamination was substantially reduced, but not completely eliminated, after heating the samples at 200 °C under vacuum for 24 hours. The generalized PDOS of $BaBiO_3$ and $Ba_{0.6}K_{0.4}BiO_3$ were also measured at 200 and 100 K and were found to be essentially identical to the room temperature data. Figure 2 shows the spectral distribution functions $P(\bar{\alpha},\beta)$ (equation (1)) between 0 and 100 meV for $BaBiO_3$ and $Ba_{0.6}K_{0.4}BiO_3$ in down-scattering mode at 5 K. Data were also collected at 45 K (i.e. just above the temperature of zero resistance in the superconductor) and as is demonstrated in figure 3, there is no discernible difference in the phonon spectrum of the superconducting sample above and below T_c within the resolution of our instrument.

From both molecular (MD) [13] and lattice (LD) [25, 30] dynamics calculations, it is known that the frequencies of O-stretching vibrations towards the central metal (Pb, Bi, Sb) atoms of the octahedral units lie around 60 meV, while the O-bending modes cover a range from 10 to 35 meV. Furthermore, the frequencies of the phonon modes

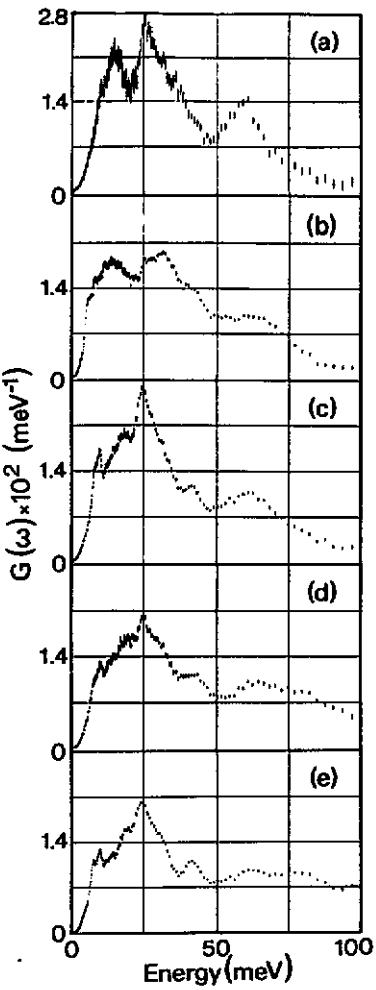

Figure 1. Generalized phonon density of states $G(\omega)$ for (*a*) $Ba_{0.6}K_{0.4}BiO_3$; (*b*) $BaBiO_3$; (*c*) $BaPb_{0.75}Bi_{0.25}O_3$; (*d*) $BaPb_{0.75}Sb_{0.25}O_3$ and (*e*) $BaPbO_3$ between 0 and 100 meV at 300 K (up-scattering mode).

arising from the A perovskite site cations are near 15 meV, while the vibrations of the B-site cations reach values of up to 20 meV.

The phonon spectrum of $Ba_{0.6}K_{0.4}BiO_3$ is relatively simple and is characterized by the presence of three very broad peaks at energies 15, 25 (actually a doublet at 24.5 and 26.5 meV) and 60.5 meV at 300 K. Weaker features are also observable at 10.5, 31.5, 36, 44, 55.5 and 68 meV. No phonon feature shows any significant temperature dependence. The high-energy bands are undoubtedly related to the O-breathing phonons [16,25,30], while zone-centre T_{1u} (IR-active) and T_{2u} (silent) modes are expected in the vicinity of the 25 meV energy range [31]. It is tempting to assign the two features at 24.5 and 26.5 meV to these T_{1u} and T_{2u} modes, respectively. At lower energies, the band at 15 meV has a remarkably high intensity compared to the other perovskite compounds studied (*vide infra*); this region involves primarily external modes with strong motion of the (Ba, K) ions as well as rotational modes. The

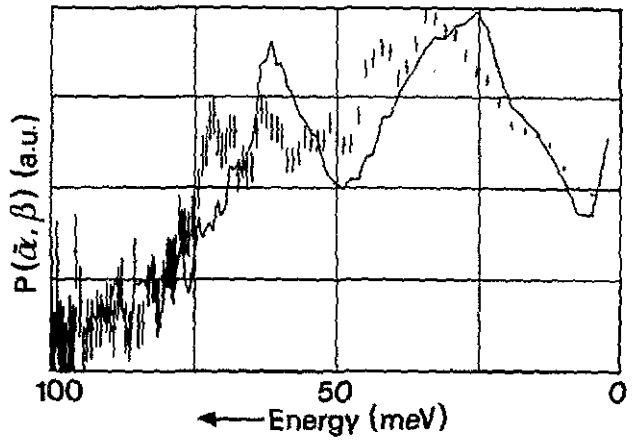

Figure 2. Measured spectral distribution $P(\tilde{\alpha},\beta)$ for $Ba_{0.6}K_{0.4}BiO_3$ (full curve) and $BaBiO_3$ (+++) at 5 K (down-scattering mode).

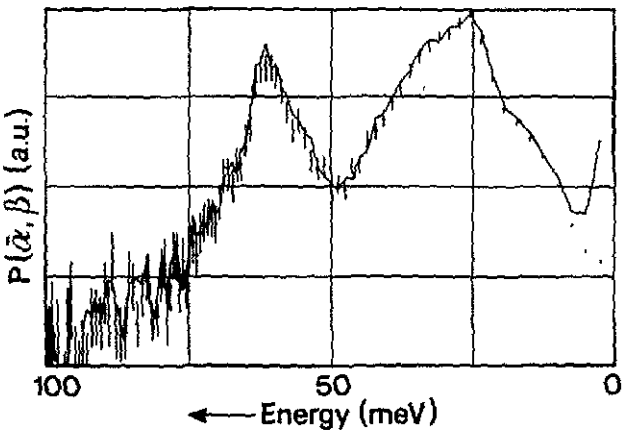

Figure 3. Measured spectral distribution $P(\tilde{\alpha},\beta)$ for $Ba_{0.6}K_{0.4}BiO_3$ above (45 K, +++) and below (5 K, full curve) the superconducting transition temperature.

low-energy tail in the generalized PDOS clearly shows the presence of zone boundary phonons at 10.5 meV with evidence of marked deviations from a Debye-like ω^2 dependence with several structures, presumably arising from soft rotational phonons, apparent in the PDOS. Figure 4(*a*) shows the 0–40 meV expanded portion of the PDOS of $Ba_{0.6}K_{0.4}BiO_3$.

The phonon spectrum of $BaBiO_3$, on the other hand, is considerably richer in structure. This is to be expected since $BaBiO_3$ adopts a monoclinic structure, resulting from a combination of the orthorhombic distortion of the perovskite unit cell and the freezing of the breathing mode of the BiO_6 octahedra. The low-temperature results in down-scattering mode (figure 2) reveal a double-peak structure in the PDOS both in the O-breathing and the O-bending regions of the spectrum in sharp contrast to the single-peak pattern apparent in the PDOS of $Ba_{0.6}K_{0.4}BiO_3$. The major peaks occur at 71.5 and 63 meV, and again at 42 and 34 meV. In both regions the peaks show substantial shifts to lower frequencies for $Ba_{0.6}K_{0.4}BiO_3$. Careful examination

of the PDOS in the up-scattering mode (figure 1(*b*)) reveals further features at 25.5 and 53 meV. The low-energy part of the phonon spectrum also appears extremely complicated with many structures apparent (at 5.8, 6.7, 8.2, 11 and 14 meV) in the region where both rotational modes of the BiO_6 octahedra and vibrations involving contributions from Ba are expected. What appears remarkable is the increased density of states in the 0–10 meV energy range compared to $Ba_{0.6}K_{0.4}BiO_3$ (*vide supra*) and the rest of the perovskites studied (*vide infra*). Temperature-dependent Raman studies of $BaBiO_3$ [26] had identified a soft rotational mode at 6 meV in excellent agreement with the substantially increased intensity observed in the PDOS at the same energy. Similarly, the 'charge disproportionation' mode has been assigned on the evidence of IR data [31] to features in the 12–13 meV energy range. Therefore, the increased intensity in the PDOS in the same range with the observation of two peaks at 11 and 14 meV may be seen as the signature of the Bi^{III}–Bi^{V} superstructure in the doubled unit cell, through folding of the Brillouin zone.

The phonon spectra of the three perovskites $BaPbO_3$, $BaPb_{0.75}Bi_{0.25}O_3$ and $BaPb_{0.75}Sb_{0.25}O_3$ recorded at room temperature between 0 and 100 meV in up-scattering mode are very similar. We may recall that $BaPbO_3$ is a metallic perovskite which adopts a monoclinic structure resulting from the tilting of the PbO_6 octahedra about the [110] direction of the pseudo-cubic perovskite unit cell [32]. Furthermore, there is only one type of PbO_6 octahedra in the structure. The structures of both $BaPb_{0.75}Bi_{0.25}O_3$ [22] and $BaPb_{0.75}Sb_{0.25}O_3$ [24] have been reported as tetragonal with single $(Pb,Bi)O_6$ and $(Pb,Sb)O_6$ octahedra rotated about the [001] direction. However, the existence of structural modifications of $BaPb_{0.75}Bi_{0.25}O_3$ has been established [23]; in the room temperature orthorhombic phase, there is a single type of octahedral unit showing a [110] tilt, identical to the case of $BaPbO_3$. On cooling, there is a phase transition to a monoclinic structure in which there are two distinct types of octahedral units, tilted about [111]. Similar detailed structural studies have not been undertaken for $BaPb_{0.75}Sb_{0.25}O_3$. The generalized PDOS of figure 1 reflect these similarities in the structures. In the low-energy transfer region, there are strong peaks at 10 meV with a pronounced shoulder at 8.6 meV and weaker features at 3.7 and 6.9 meV for all three samples. This is followed by the 11–21 meV region which is rich in structure, involving contributions from both B- and A-site atoms. The T_{1u} and T_{2u} phonons appear in the 24–25 meV region for all three samples and a shoulder is present at ca. 30 meV. At higher energies, there is a very well defined peak at 42 meV, the origin of which is difficult to explain. Reichardt and Weber [25] in their study of $BaPb_{0.75}Bi_{0.25}O_3$ assigned it to defect-type modes, associated with static distortions of the octahedral units, primarily around the Bi atoms. Shirai *et al* [30] postulated that it might still arise from the unusually broad longitudinal O-stretching mode which shows considerable energy renormalization because of the strong electron–phonon interaction. In the present study, however, the 42 meV phonon is present for both solid solutions $BaPb_{0.75}Bi_{0.25}O_3$ and $BaPb_{0.75}Sb_{0.25}O_3$ as well as the parent $BaPbO_3$ compound for which no phonon modes are expected in the 40 meV range. Furthermore, our results show that the intensity and width of this band depend on the sample; it spreads more and becomes less sharp as we move from $BaPbO_3$ to $BaPb_{0.75}Bi_{0.25}O_3$ to $BaPb_{0.75}Sb_{0.25}O_3$. This is probably related to the increased disorder and the presence of different types of locally distorted octahedra in the Bi- and Sb-doped materials. The generalized PDOS of $Ba_{0.6}K_{0.4}BiO_3$ has a much weaker feature at 44 meV that may be of the same origin. Indeed a Raman scattering study of $Ba_{0.6}K_{0.4}BiO_3$ shows the presence of an optical phonon at 43 meV with a distinctive Fano lineshape [33].

The authors proposed for the origin of this phonon the existence of BiO_n units with incomplete octahedral coordination. However, the possibility that this is the same phonon we are observing in the (Pb,Bi,Sb) perovskites is very likely in view of the significant dependence of the PDOS in this region on the level of doping. Finally, the PDOS in the energy range > 50 meV show the most pronounced differences between the three samples. (Recall, however, that there is some scattering from adsorbed water for the $BaPbO_3$ and $BaPb_{0.75}Sb_{0.25}O_3$ samples in this energy region). $BaPbO_3$ shows the presence of two peaks at 63 and 78 meV which may be assigned to the O-breathing vibrations. The intensity of the 78 meV zone-boundary phonon is found to depend strongly on the type of dopant; it is clearly present, albeit with reduced intensity, in $BaPb_{0.75}Sb_{0.25}O_3$ (T_c = 3.5 K) but has virtually disappeared for $BaPb_{0.75}Bi_{0.25}O_3$ (T_c = 13 K). This behaviour should arise as a result of the strong energy renormalization of the O-breathing phonons and provides evidence for the importance of these phonons in the superconducting mechanism [30].

4. Conclusions

The generalized ('neutron-weighted') phonon density of states (figures 1–4) has been measured by the neutron time-of-flight technique for a series of perovskites at temperatures between 5 and 300 K. Metallic $BaPbO_3$ is one end-member of this series, becoming superconducting upon introduction of either Bi or Sb on the B site. Replacement of Pb by Bi leads eventually to the semiconducting $BaBiO_3$ system, characterized by the presence of a Bi(III)–Bi(V) charge density wave, resulting from the freezing of the O-breathing vibrations at the R point. Doping of $BaBiO_3$ on the A site by K^+ leads again to a superconducting composition which currently has the highest superconducting transition temperature known for a non-copper-containing oxide. Our results broadly agree with the IR, Raman and neutron scattering studies of these systems that have appeared in the literature before. However, by systematically covering a more extensive range of systems at different temperatures and at better resolution especially near the elastic peak, a number of novel points have been revealed.

Starting from $BaPbO_3$ as our reference system, the neutron scattering measurements reveal no discernible differences betwen the parent system and the two superconductors, $BaPb_{0.75}Bi_{0.25}O_3$ and $BaPb_{0.75}Sb_{0.25}O_3$ in their PDOS up to the bond-stretching O-breathing phonon energy region. However, the high frequency part of the PDOS distribution is considerably affected, demonstrating the importance of these phonons in the electron–phonon coupling mechanism in the superconducting oxides. Furthermore, we find evidence of differences in the magnitude of the electron–lattice interaction between $BaPb_{0.75}Bi_{0.25}O_3$ and $BaPb_{0.75}Sb_{0.25}O_3$ as revealed by the behaviour of the 78 meV zone-boundary O-breathing phonon; it shifts to lower energy and its intensity is reduced in the Sb-doped oxide and totally disappears in the Bi-doped one. This result provides an explanation for the reduction of T_c from 13 to 3.5 K within a phonon-mediated mechanism of superconductivity, implying that λ decreases on going from Bi to Sb. It also implies that phonon modes away from the Brillouin zone centre seem to be important for the electron–lattice interaction mechanism. A further point of interest within this series of oxides is the observation of a phonon at 42 meV, an energy region where no phonon branch is expected by lattice dynamics calculations. This was rationalized before in the Bi system [25] by invoking the presence of lattice defect vibrational modes, associated with locally distorted octahedral

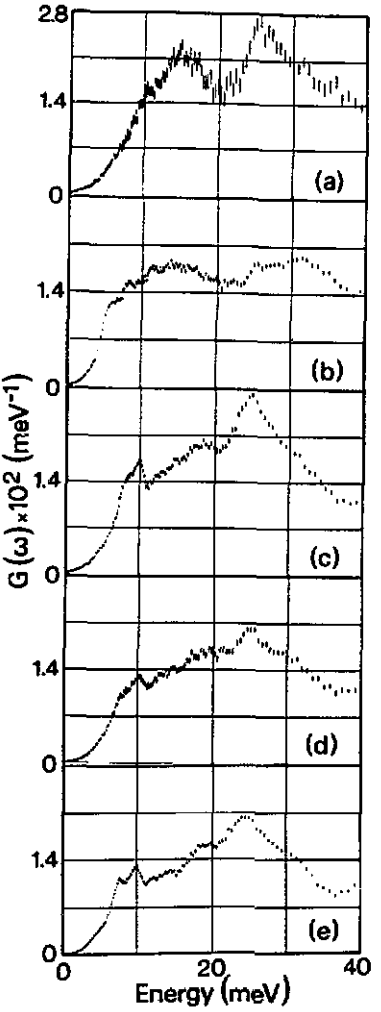

Figure 4. generalized phonon density of states $G(\omega)$ for (*a*) $Ba_{0.6}K_{0.4}BiO_3$; (*b*) $BaBiO_3$, (*c*) $BaPb_{0.75}Bi_{0.25}O_3$; (*d*) $BaPb_{0.75}Sb_{0.25}O_3$ and (*e*) $BaPbO_3$ between 0 and 40 meV at 300 K (up-scattering mode).

units; this explanation has been questioned subsequently [30, 33]. Our experimental data support the presence of such defects in both the parent and the doped materials; we find that the intensity and width of the 42 meV peak is dependent on the perovskite sample, being more sharp and well-defined in $BaPbO_3$ than the Bi and Sb doped systems. This is consistent with the presence of a larger spread of distorted octahedra in the doped oxides, and even more so in the Sb system.

The generalized PDOS of the mixed valency $BaBiO_3$ compound proves to be much more complicated as a result of both the superstructure formation due to charge disproportionation and the tilting of the octahedra. There is also increased DOS in the low-energy transfer region, presumably associated with soft rotational modes. Doping on the A site ($Ba_{0.6}K_{0.4}BiO_3$) leads to substantial lowering of both the O-breathing and O-bending vibrational modes, in agreement with earlier reports [16]. The domi-

nance of such high-energy phonon modes in the electron–phonon coupling mechanism is revealed in the LD calculations [30] and can explain the unusual temperature dependence of the thermoelectric power of $Ba_{0.6}K_{0.4}BiO_3$ [34]. Both calculated [35] and experimental tunnelling [15] spectra also support these conclusions. Furthermore, the low-energy part of the spectrum is very simple with main peaks at 15 (of unusually high intensity) and 10.5 meV, consistent with the cubic structure and the suppression of both the CDW and the tilting of the octahedra.

No changes in the PDOS have been observed when the sample was cooled down past its T_c of 30 K. This finding is not in contradiction with an electron–phonon coupling mechanism for superconductivity since it has been found by Raman scattering that both positive and negative shifts of optical phonon frequencies can occur in high-T_c materials [36]. This behaviour was predicted for optical zone-centre phonons using strong coupling theory [37]. Furthermore, it is likely that the moderate energy resolution (6–4 meV) does not allow the expected small shifts (0.1–0.2 meV) to be revealed. In the cuprate superconductors, phonon anomalies are found in the oxygen vibrations region of the PDOS but they are much more subtle and have proved difficult to directly relate to the superconductivity mechanism. In contrast, it appears that the importance of phonons is much more pronounced in the perovskite superconductors with phonon anomalies directly related to the strength of the electron–phonon coupling and the magnitude of the superconducting transition temperature.

Acknowledgments

This work is supported by the Science and Engineering Research Council (KP). We thank the Institut Laue Langevin for provision of neutron beam time. MJR is a Junior Research Fellow at Merton College, Oxford.

References

[1] Bednorz J G and Müller K A 1986 *Z. Phys.* B **64** 189
[2] Tokura Y, Takagi H and Uchida S 1989 *Nature* **337** 345
[3] Rosseinsky M J, Prassides K and Day P 1989 *J. Chem. Soc. Chem. Commun.* 1734; 1991 *Inorg. Chem.* **30** 2680
[4] Day P, Rosseinsky M J, Prassides K, David W I F, Moze O and Soper A 1987 *J. Phys. C: Solid State Phys.* **20** L429
Rosseinsky M J, Prassides K and Day P 1991 *J. Mater. Chem.* **1** 597
[5] Paul D McK, Balakrishnan G, Bernhoeft N R, David W I F and Harrison W T A 1987 *Phys. Rev. Lett.* **58** 1976
[6] David W I F *et al* 1987 *Nature* **327** 310
[7] Sawa H, Suzuki S, Watanabe M, Akimitsu J, Kolcirlo K, Asaio H, Izuki F and Takayama-Muromachi E 1989 *Nature* **337** 347
[8] Birgeneau R J, Kastner M A and Aharony A 1987 *Z. Phys.* B **68** 425
Aharony A, Birgeneau R J, Coniglio A, Kastner M A and Stanley H E 1988 *Phys. Rev. Lett.* **60** 1330
[9] Luke G M *et al* 1989 *Nature* 338 49; 1990 *Phys. Rev.* B **42** 7981
Endoh Y, Matsuda M, Yamada K, Kakurai K, Hidaka Y, Shirane G and Birgeneau R J 1989 *Phys. Rev.* B **40** 7023
Skanthakumar S, Zhang H, Clinton T W, Li W-H, Lynn J W, Fisk Z and Cheong S-W 1989 *Physica* C **160** 124
[10] Rosseinsky M J, Prassides K, Day P and Dianoux A J 1988 *Phys. Rev.* B **37** 2231

[11] Renker B, Gompf F, Gering E, Nucker N, Ewert D, Reichardt W and Rietschel H 1987 *Z. Phys.* B **67** 15
Renker B, Gompf F, Gering E, Ewert D, Rietschel H and Dianoux A J 1988 *Z. Phys.* B **73** 309
Strobel P, Monceau P, Tholence J L, Currat R, Dianoux A J, Capponi J J and Bednorz J G 1989 *Physica* C **153–155** 282
Belushkin A V, Goremychkin E A, Nathaniec I, Sashin I L and Zajac W 1989 *Physica* C **156–157** 906
[12] Currat R, Dianoux A J, Monceau P and Capponi J J 1989 *Phys. Rev.* B **40** 11362
Dianoux A J, Currat R, Strobel P, Monceau P, Capponi J J, Tholence J L and Femandez-Diaz M T 1990 *Proc. Int. Seminar on High Temperature Superconductivity* vol 21 (London: World Scientific) p 305
[13] Loong C-K *et al* 1989 *Phys. Rev. Lett.* **62** 2628
[14] Mattheiss L F, Gyorgy E M and Johnson D W Jr 1988 *Phys. Rev.* B **37** 3745
Cava R J, Batlogg B, Krajewski J J, Farrow R, Rupp L W Jr, White A E, Short K, Peck W F and Kometani T 1988 *Nature* **332** 814
Hinks D G, Dabrowski B, Jorgensen J D, Mitchell A W, Richards D R, Pei S and Shi D 1988 *Nature* **333** 836
[15] Zasadzinski J F, Tralshawala N, Hinks D G, Dabrowski B, Mitchell A W and Richards D R 1989 *Physica* C **158** 519
Huang Q, Zasadzinski J F, Tralshawala N, Gray K E, Hinks D G, Peng J L and Greene R L 1990 *Nature* **347** 369
[16] Loong C-K *et al* 1991 *Phys. Rev. Lett.* **66** 3217
[17] Batlogg B, Cava R J, Rupp L W Jr, Mujsce A M, Remeika J P, Peck W F Jr, Cooper A S and Espinosa G P 1988 *Phys. Rev. Lett.* **61** 1670
[18] Sleight A W, Gilson J L and Bierstedt P E 1975 *Solid State Commun.* **17** 27
[19] Itoh T, Kitazawa K and Tanaka S 1984 *J. Phys. Soc. Japan.* **53** 2668
[20] Cox D E and Sleight A W 1979 *Acta Crystallogr.* B **35** 1
[21] For recent reviews on the subject, see for example:
Prassides K (ed) 1991 *Mixed Valency Systems: Applications in Chemistry, Physics and Biology* (Dordrecht: Kluwer)
[22] Cox D E and Sleight A W 1976 *Proc. Int. Conf. on Neutron Scattering (Gatlinburg, 1976)* p 45
[23] Asano H, Oda M, Endoh Y, Hidaka Y, Izumi F, Ishigaki T, Karahashi K, Murakami T and Watanabe N 1988 *Japan. J. Appl. Phys.* **27** 1638
Rosseinsky M J and Prassides K unpublished results
[24] Cava R J, Batlogg B, Espinosa G P, Ramirez A P, Krajewski J J, Peck W F Jr, Rupp L W Jr and Cooper A S 1989 *Nature* **339** 291
[25] Reichardt W, Batlogg B and Remeika J P 1985 *Physica* B 501
Reichardt W and Weber W 1987 *Japan. J. Appl. Phys. Suppl.* 3 **26** 1121
[26] Sugai S, Uchida S, Kitazawa K, Tanaka S and Katsui A 1985 *Phys. Rev. Lett.* **55** 426
Sugai S 1987 *Japan. J. Appl. Phys. Suppl.* 3 **26** 1123
[27] Masaki A *et al* 1987 *Japan. J. Appl. Phys.* **26** L405
[28] Egelstaff P A and Schofield P 1962 *Nucl. Sci. Eng.* **12** 260
[29] Dianoux A J and Currat R unpublished
[30] Shirai M, Suzuki N and Motizuki K 1990 *J. Phys.: Condens. Matter* **2** 3553
[31] Uchida S, Tajima S, Masaki A, Sugai S, Kitazawa K and Tanaka S 1985 *J. Phys. Soc. Japan.* **54** 4395
[32] Ritter H, Ihringer J, Maichle J K, Prandl W, Hoser A and Hewat A W 1989 *Z. Phys.* B **75** 297
[33] McCarty K F, Radousky H B, Hinks D G, Zheng Y, Mitchell A W, Folkerts T J and Shelton R N 1989 *Phys. Rev.* B **40** 2662
[34] Uher C, Peacor S D and Kaiser A B 1991 *Phys. Rev.* B **43** 7955
[35] Shirai M, Suzuki N and Motizuki K 1990 *Solid State Commun.* **73** 633
[36] Thomsen C, Cardona M, Friedl B, Rodriguez C O, Mazin I I and Andersen O K 1990 *Solid State Commun.* **75** 219
Altendorf E, Chrzanowski J, Irwin J C, O'Reilly A and Hardy W N 1991 *Physica* C **175** 47
[37] Zeyher R and Zwicknagl G 1990 *Z. Phys.* B **78** 175